ONLINE SUPPLEMENT

Akt2 Stabilizes ATP7A, a Cu transporter for SOD3, in Vascular Smooth Muscles: Novel Mechanism to Limit Endothelial Dysfunction in Type2 diabetes

Varadarajan Sudhahar[1,2,5,7,11], Mustafa Nazir Okur[6], Zsolt Bagi[1,3], John P O'Bryan[6,7], Nissim Hay[9], Ayako Makino[10], Vijay S Patel[4], Shane A Phillips[8], David Stepp[1], Masuko Ushio-Fukai[1,3,6,7],*Tohru Fukai,[1,2,5,7,11,12]

[1]Vascular Biology Center, [2]Departments of Pharmacology and Toxicology, and [3]Medicine (Cardiology), [4] Department of Surgery, Medical College of Georgia at Augusta University, Augusta, GA. [5]Departments of Medicine (Cardiology) and Pharmacology, [6]Department of Pharmacology, [7]Center for Cardiovascular Research, [8]Department of Physical Therapy, [9]Department of Biochemistry and Molecular Genetics, University of Illinois at Chicago, [10]Department of Medicine and Physiology, University of Arizona. [11]Jesse Brown Veterans Affairs Medical Center, Chicago IL [12]Charlie Norwood Veterans Affairs Medical Center, Augusta GA

Address correspondence to:

Tohru Fukai, M.D., Ph.D.
Vascular Biology Center
Department of Pharmacology and Toxicology
Medical College of Georgia at Augusta University
1459 Laney-Walker Blvd,
Augusta, GA 30912, USA
Phone: 706-721-6380
Email: tfukai@augusta.edu

Supplementary Tables

	Control	**T2DM**
Body weight, g	32.5±1.45	49.9±5.43*
Glucose, mg/dl	175 ± 3.02	268 ± 15.1*
Total Triglycerides, mg/dl	135 ± 27.9	483 ± 43.2*
Total cholesterol, mg/dl	68.87 ± 4.15	179.5 ± 9.28*
HDL, mg/dl	38.35 ± 4.03	83.11 ± 6.01*
LDL+VLDL, mg/dl	27.44 ± 7.11	92.50± 3.62*
HOMA-IR	4.41 ± 0.23	32.86 ± 4.16*

Supplemental Table I. Metabolic characterization of control and diabetic mice. Plasma triglyceride and cholesterol levels were measured in mice after overnight fasting according to manufacturer instructions as showed in method section. n= 20 mice in each group. Results are presented as mean ± SEM. *p<0.05.

Characteristics	Non-DM	DM
Total	n=7	n=8
Age, Years (Mean ± SEM)	59.7 ± 4.4	62 ± 1.9
Body Mass Index (Mean ± SEM)	27.3 ± 1.0	41.1 ± 4.0
Sex, Male/Female	6/1	4/4

Supplemental Table II. Patient Demographics

Supplementary Figures

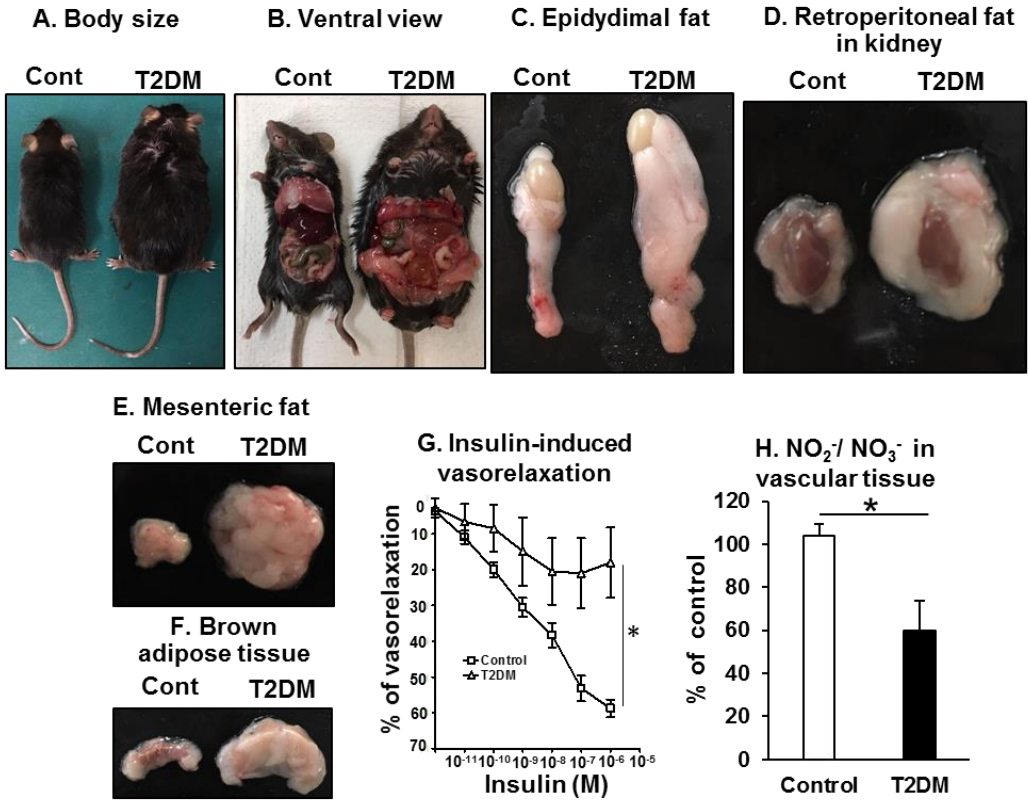

Supplementary Figure I. Characterization of high fat diet (HFD)-induced T2DM mice. T2DM was induced by 12-16 week of high fat (60% kcal) diet combined with single injection of low dose streptozotocin (STZ). **A,** Representative images of body size. **B,** Exposed ventral view of mice. **C-F,** HFD-induced T2DM mice showed a substantial increase in the size of fat pads from various adipose tissue compared with control mice. **G,** Isometric tension of mesenteric resistance arteries from HFD-T2DM or control mice was measured in isolated organ chambers using a wire myograph. Vasodilation was evoked by insulin after preconstriction with phenylephrine (1–5 μmol/L). **H,** Nitrate/nitrite levels was measured in HFD-T2DM (n=6) mice using Nitrate/nitrite colorimetric assay (Cayman chemicals). Results are presented as mean ± SEM. *p<0.05, *NS*, not significant.

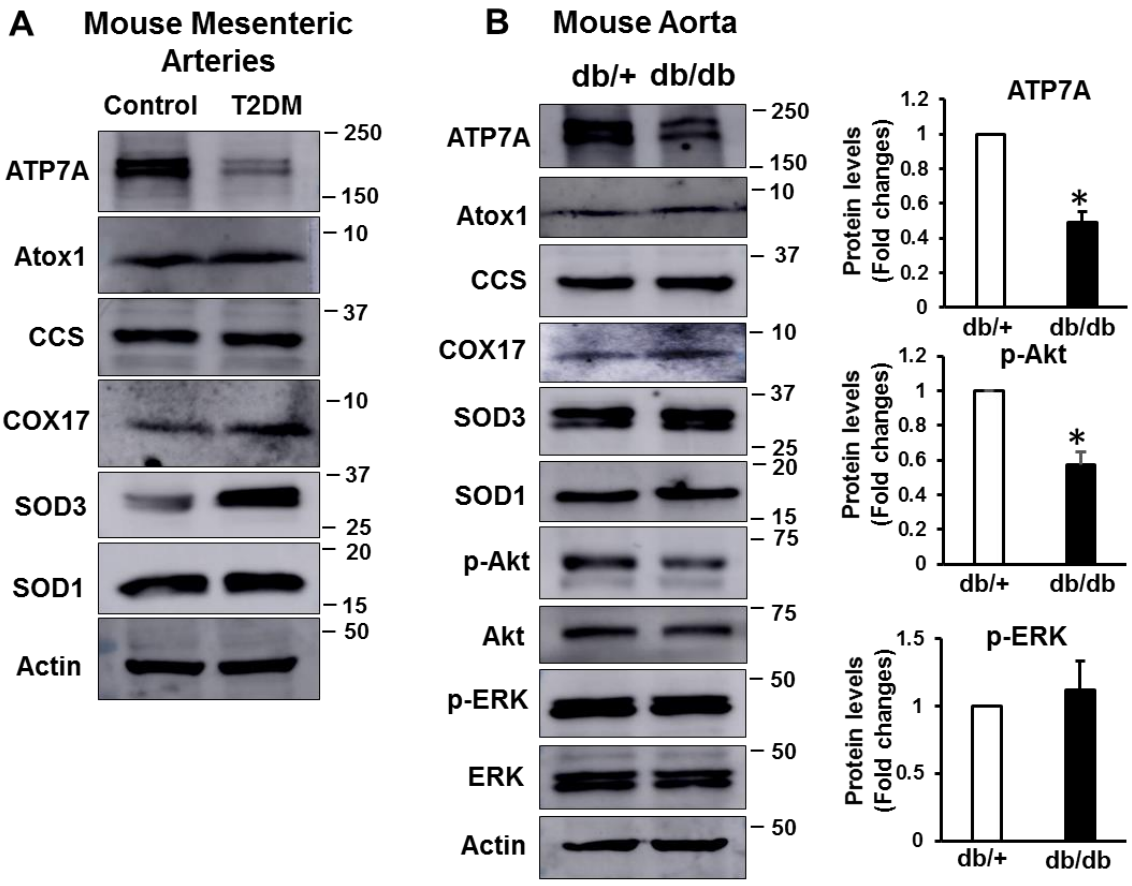

Supplementary Figure II. Protein expression of ATP7A, but not other copper transport proteins, is decreased in mesenteric arteries from HFD-induced T2DM mice (A) as well as in aortas from genetically-induced T2DM db/db mice (B). A and B, Indicated protein levels were determined by immunoblot (n=3). Right panel, densitometry analysis was shown. (n=3).

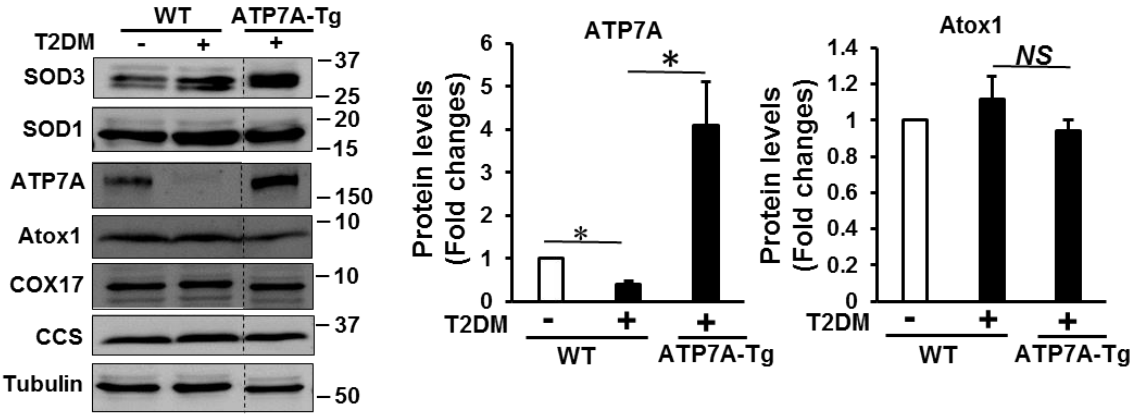

Supplementary Figure III. Protein expression for ATP7A, Atox1, CCS, and COX17 in aorta of control or diabetic or diabetic transgenic mice overexpressing ATP7A mice (n=4). Results are presented as mean ± SEM. *p<0.05, *NS*, not significant.

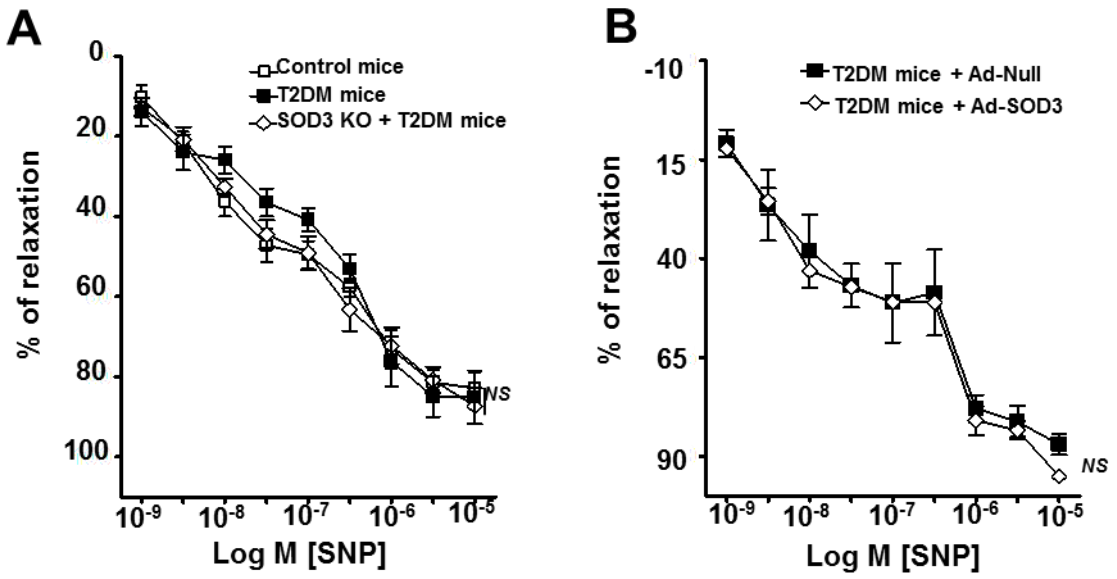

Supplementary Figure IV. SNP-mediated endothelium-independent vasodilation is not altered in mesenteric arteries of T2DM or T2DM SOD3$^{-/-}$ mice or T2DM mice with SOD3 gene transfer. Isometric tension of mesenteric resistance arteries from control, T2DM WT, T2DM SOD3$^{-/-}$ mice (A) T2DM mice with SOD3 gene transfer (B) was measured in isolated organ chambers using a wire myograph. Vasodilation was evoked by SNP after preconstriction with phenylephrine (1–5 µmol/L) (n=5-8). Results are presented as mean ± SEM. *NS*, not significant.

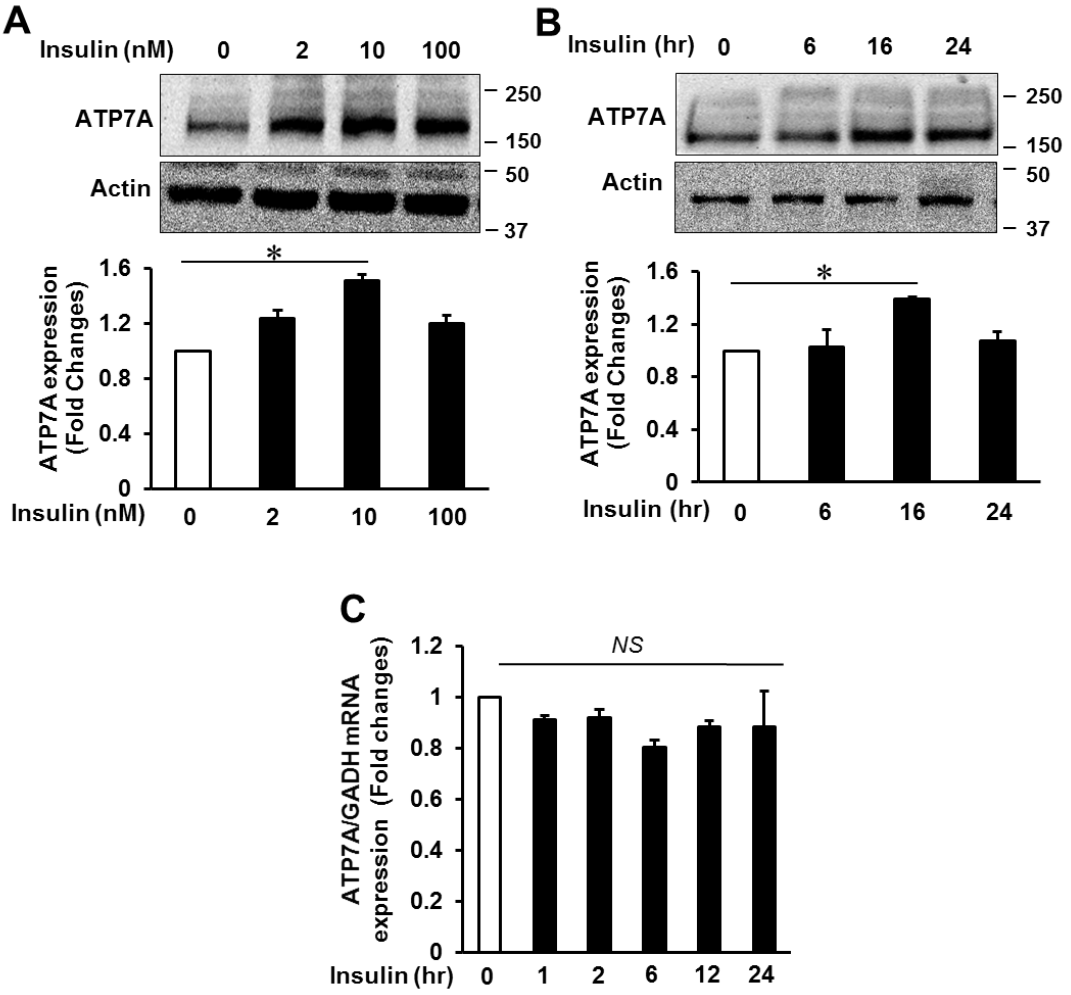

Supplementary Figure V. Insulin increases ATP7A protein expression without affecting ATP7A mRNA expression in a dose- and time- dependent manner in VSMCs. A and B, Rat VSMCs (RASMs) treated with insulin as indicated dose (A) as well as time (B) were immunoblotted with anti-ATP7A antibody. Bottom, averaged data for ATP7A protein, expressed as fold changes of unstimulated VSMCs (n=4). **C,** quantitative real-time PCR analysis of ATP7A mRNA expression in RASMs treated with insulin (10 nM) at different time points (n=4). GAPDH mRNA levels were used as internal control. Results are presented as mean ± SEM. *p<0.05. *NS*, not significant.

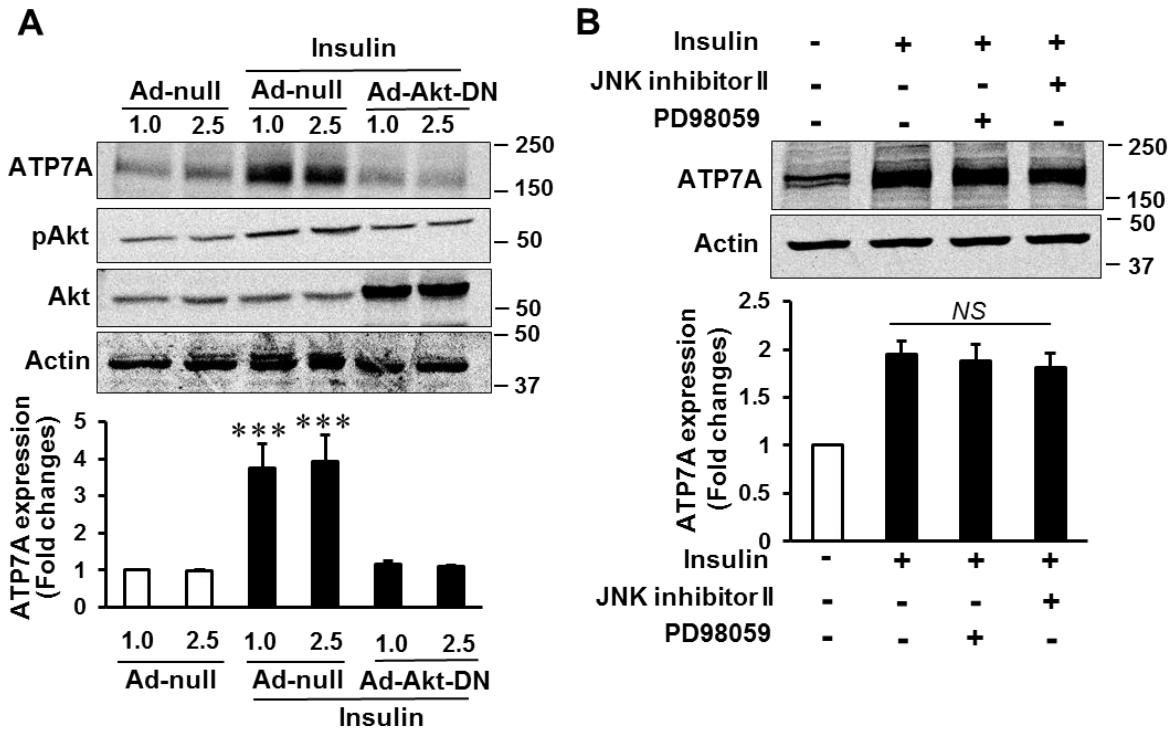

Supplementary Figure VI. Akt, but not ERK or JNK, is involved in insulin-induced ATP7A protein expression in VSMCs. A, RASMs infected with Adeno-Akt dominant negative (Akt-DN) were stimulated with insulin (10 nM, 16 hrs) and lysates were used to measure ATP7A, Akt and actin proteins (n=4). **B,** RASMs treated with JNK inhibitor II (20 uM) or ERK inhibitor, PD98059 (10uM) for 30min were stimulated with insulin (10 nM, 16 hrs). Lysates were used to measure ATP7A protein expression. Bottom, averaged data for ATP7A protein, expressed as fold changes of unstimulated VSMCs (n=4). Results are presented as mean ± SEM. *NS*, not significant.

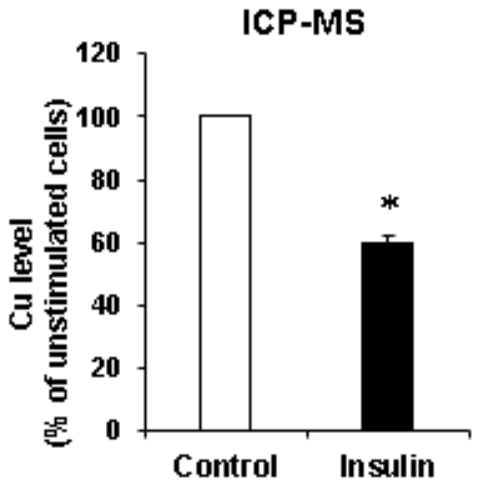

Supplementary Figure VII. Effect of insulin on Cu levels in VSMCs. Copper contents were measured by ICP-MS in cell lysates of RASMs stimulated with or without insulin (10 nM) for 16 hrs (n=4). Results are presented as mean ± SEM. *$p<0.05$.

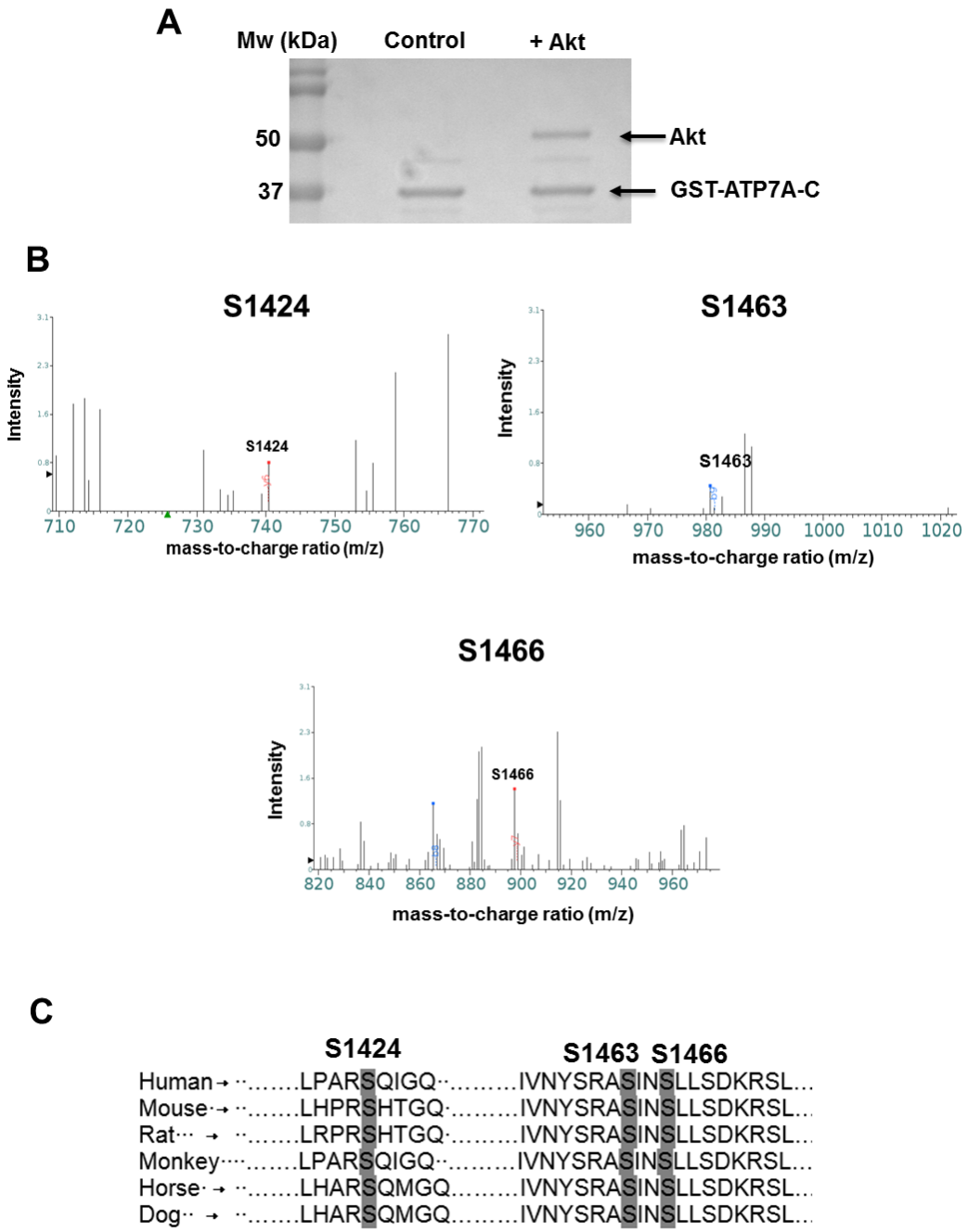

Supplementary Figure VIII. Identification of Akt-induced phosphorylation site in ATP7A by tandem mass spectrometry analysis. A, C-terminus ATP7A-GST proteins incubated with 50 μM ATP in kinase buffer with or without recombinant Akt protein were stained with Coomassie Blue. Arrows denote the position of GST-C-Terminus ATP7A and Akt. **B**, GST-C-terminus ATP7A proteins after in vitro kinase assay were size-separated by SDS-PAGE and visualized by Coomassie blue staining. The gel containing the GST-C-terminus ATP7A protein was isolated and subjected to mass spectrometry analysis. The Akt dependent phosphorylation sites identified are S1424, S1463 and S1466. **C**, Alignment of conserved amino acids in C-terminus of ATP7A at different species.

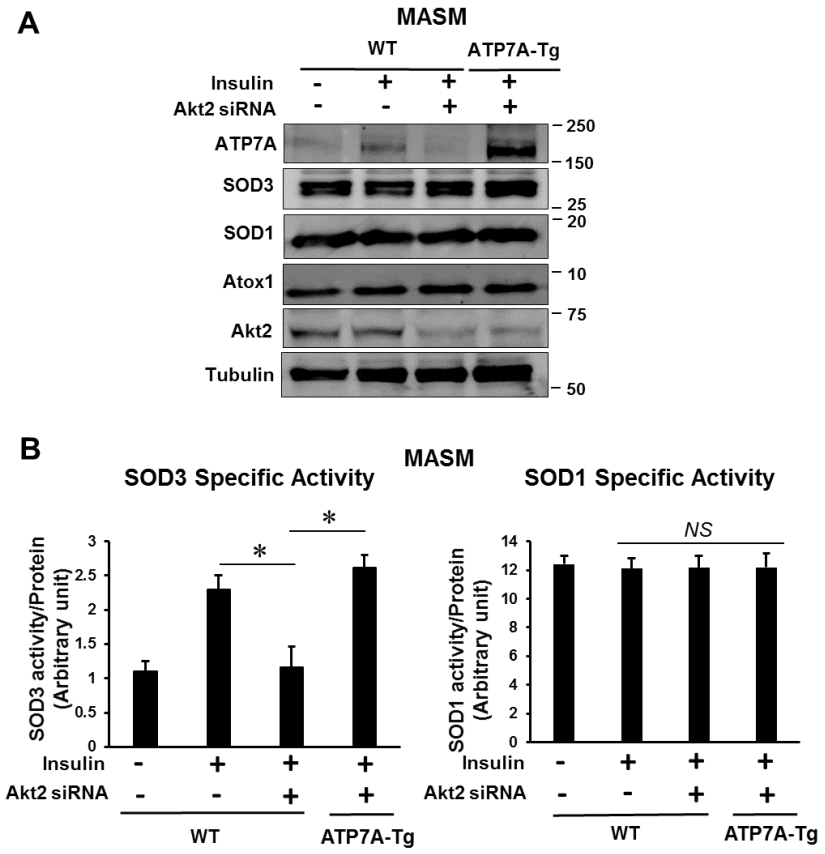

Supplementary Figure IX. Akt 2 is involved in insulin-induced ATP7A protein expression which results in activation of SOD3 secreted in the culture medium from VSMCs. Mouse aortic SMC (MASM) isolated from transgenic mice overexpressing ATP7A or WT mice were transfected with control siRNA or Akt2 siRNA and stimulated with insulin (10nM for 48hrs). **A,** Protein expression for ATP7A, Atox1, SOD3, SOD1, Akt2 and tubulin in VSMCs. **B,** SOD3 secreted in the culture medium was collected at 48 hrs after addition of insulin (10 nM) and concentrated by Concanavalin-A sepharose chromatography. Activities of SOD3 and SOD1 were assayed in conditional medium as shown in Figure 2 (n=4). Results are presented as mean ± SEM. *p<0.05. NS, not significant.

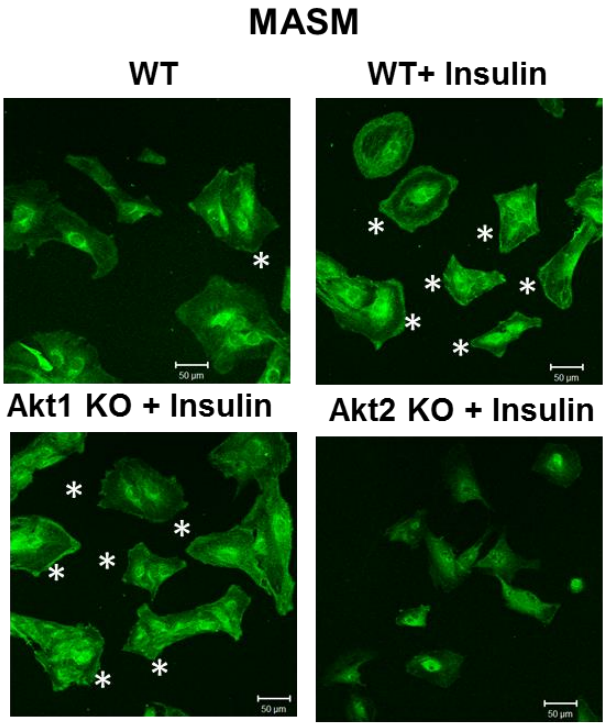

Supplementary Figure X. Insulin-induced ATP7A translocation to plasma membrane was inhibited in VSMCs isolated from Akt2 KO mice, but not those from Akt1 KO or WT mice. VSMCs isolated from Akt1 or Akt2 KO or WT mouse aorta were stimulated with insulin (10 nM, 2 hrs) and stained with anti-ATP7A. Small white stars point to the ATP7A at the plasma membrane. Bar represents 50 μm. Negative control staining lacking the anti-ATP7A primary antibody is shown in Figure XIV in the online-only Data Supplement.

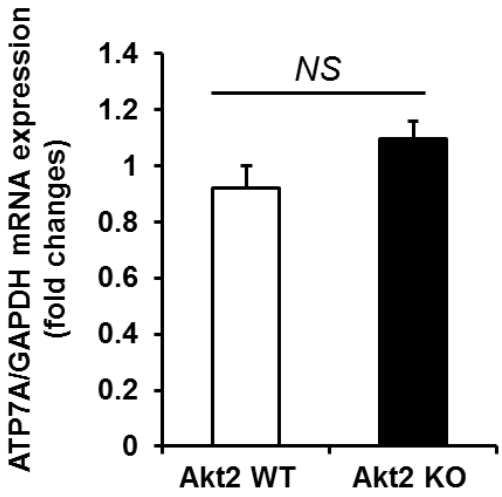

Supplementary Figure XI. ATP7A mRNA expression is not changed in the aorta of Akt2 KO mice. ATP7A mRNA expression was measured by quantitative real time PCR analysis, and GAPDH mRNA levels were used as internal control (n=4). NS, not significant.

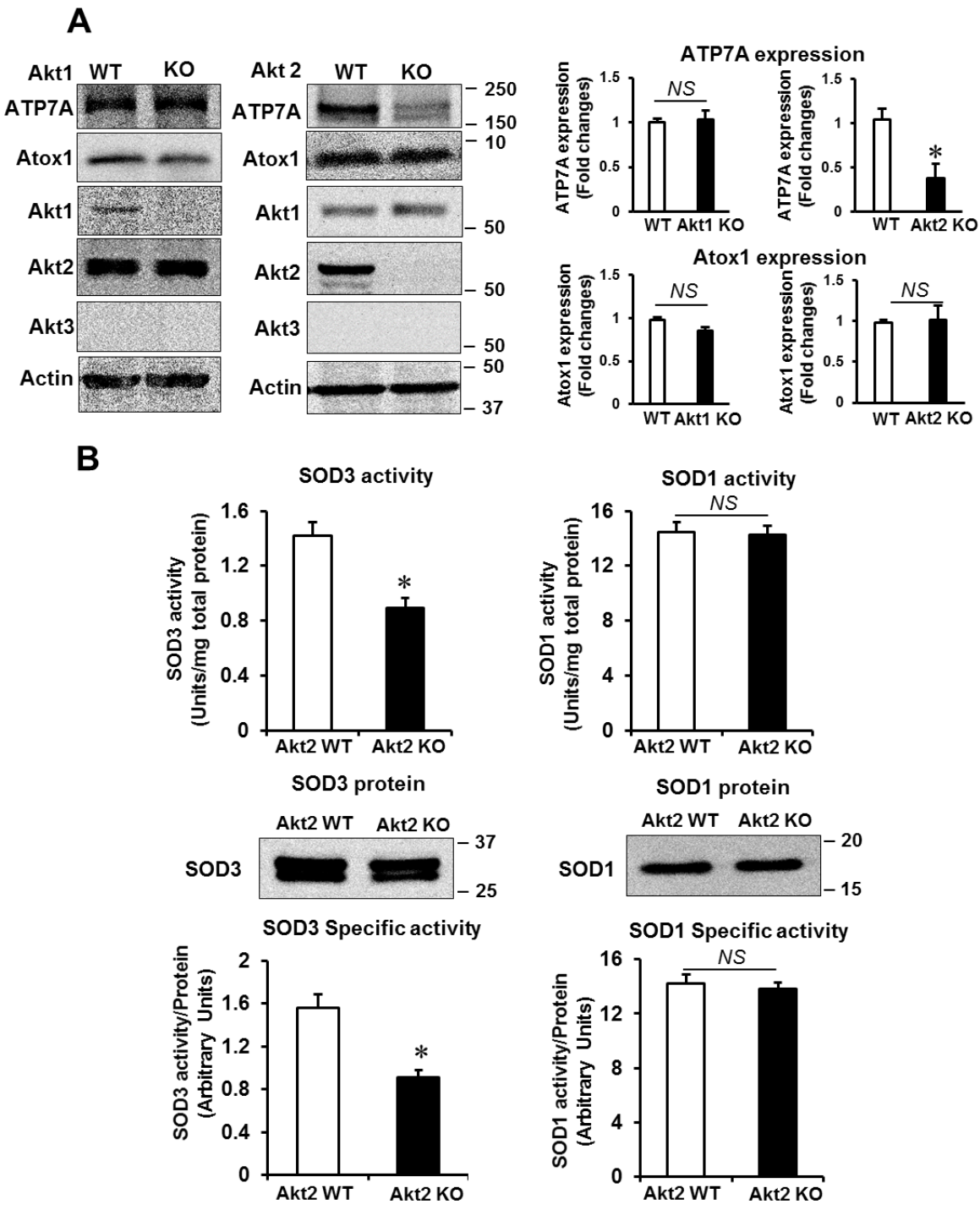

Supplementary Figure XII. Male Akt2$^{-/-}$ mice show decrease in ATP7A protein expression and specific SOD3 activity in vascular tissue. A, Protein expression for ATP7A and Atox1 in the aortas of male Akt1 or Akt2 KO mice (n=4). **B,** Top panel, activities of SOD3 and SOD1 in homogenates from male Akt2 KO or WT mouse aorta as shown in Figure 2. Middle panel, protein levels of SOD1 and SOD3. Bottom panel, specific activities of SOD1 and SOD3 was determined by the ratio of activity to the relative amount of protein (n=4). Results are presented as mean ± SEM. *p<0.05. NS, not significant.

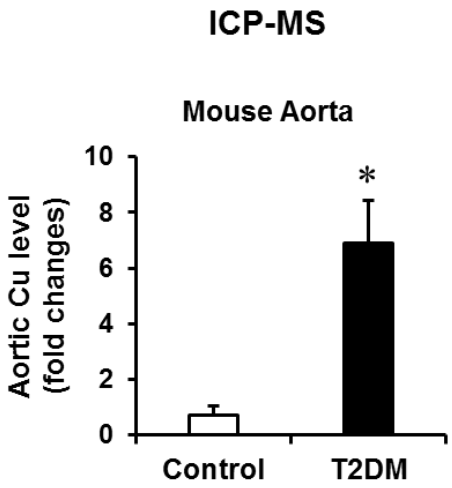

Supplementary Figure XIII. Cu levels in aortas from T2DM mice. Aortic copper content in T2DM and control mice was measured by inductively coupled plasma mass spectrometry (ICP-MS). Data are quantified using 4 samples for each group and presented as mean ± SEM. *$p<0.05$.

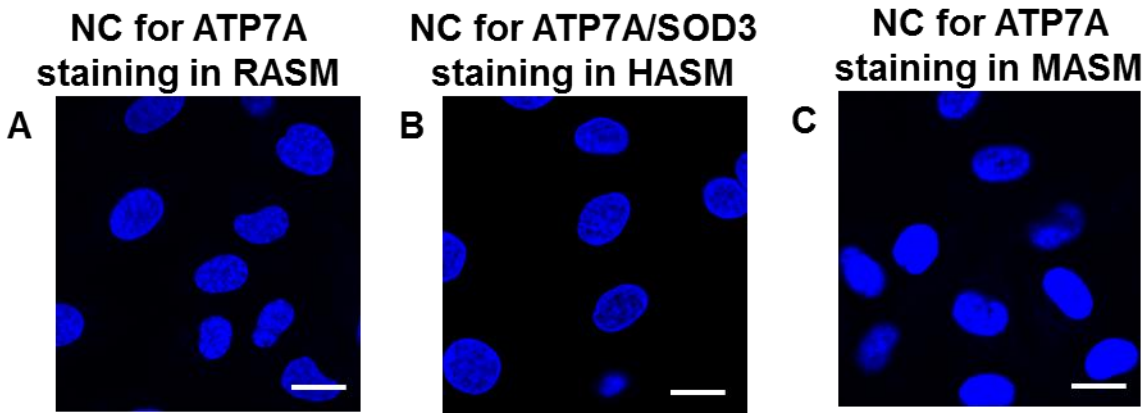

Supplementary Figure XIV. Negative control (NC) staining lacking the anti-ATP7A primary antibody in RASM (A) and MASM (C) as well as lacking ATP7A/SOD3 primary antibodies in HASM (B). DAPI (blue) was used to confirm the presence of cells. We used DAPI (blue) to confirm the presence of cells. Bar represents 20 μm.